"Rewiring" Filterbanks for Local Fourier Analysis: Theory and Practice

Keigo Hirakawa, *Member, IEEE*, and Patrick J. Wolfe, *Senior Member, IEEE*

Abstract— This article describes a series of new results outlining equivalences between certain "rewirings" of filterbank system block diagrams, and the corresponding actions of convolution, modulation, and downsampling operators. This gives rise to a general framework of reverse-order and convolution subband structures in filterbank transforms, which we show to be well suited to the analysis of filterbank coefficients arising from subsampled or multiplexed signals. These results thus provide a means to understand *time-localized* aliasing and modulation properties of such signals and their subband representations— notions that are notably absent from the global viewpoint afforded by Fourier analysis. The utility of filterbank rewirings is demonstrated by the closed-form analysis of signals subject to degradations such as missing data, spatially or temporally multiplexed data acquisition, or signal-dependent noise, such as are often encountered in practical signal processing applications.

Index Terms— Aliasing, likelihood methods, modulation, multiplicative noise, sampling, signal enhancement, time-frequency analysis, wavelets.

I. INTRODUCTION

Since the earliest days of signal and waveform analysis, engineers have recognized the wide utility of parameterized families of *filters*: convolution operators that are directly represented by finite-length sequences of real numbers. Parallel banks of such finite-impulse-response filters, including short-time Fourier and wavelet transforms, have long been a canonical tool for analyzing signals, images, and other data sets that arise in a variety of applications across scientific fields [1], [2]. The purpose of this article is to further expand filterbank theory and practice by developing a general framework of reverse-order and convolution subband structures in filterbank transforms. It describes a series of new results outlining equivalences between certain "rewirings" of filterbank block diagrams, and the "localized" aliasing and modulation properties of sampled signals and their subband representations, which we describe below.

Sampled signals are typically acquired as linear functionals of the underlying data object of interest, which in turn is defined with respect to a continuous variable such as time or space. The actions of the convolution operators that comprise filterbanks are studied through their Fourier transforms, under the correspondence of element-wise multiplication on the dual

group. Since sampling a continuous-time function periodizes its Fourier transform, however, care must be taken that no information is lost in the process. Indeed, in the absence of additional assumptions, it is not in general possible to recover signals that have *aliased*; that is, signals whose Fourier transforms are supported on intervals so large that this periodization mixes distinct Fourier coefficients.

As the bandwidth of any function is directly determined by its *global* smoothness, Fourier analysis does not lend itself to a meaningful analysis of signals whose smoothness varies and hence are not low-pass *everywhere*. In contrast, parallel banks of convolution operators with finite support are fundamentally *local* in nature. It is well known, for instance, that the flexibility afforded by wavelets to adapt to the local regularity of functions is essential in yielding the sparsity properties necessary for effective signal and image analysis, as well as contemporary signal acquisition techniques such as compressed sensing [3]–[8].

Filterbanks are hence essential engineering tools for data analysis. However, definitions of aliasing and frequency modulation in the global, Fourier context preclude the closed-form filterbank analysis of signals subject to missing data, spatially or temporally multiplexed acquisition, or signal-dependent noise effects. While it is well known how to apply filterbanks to analyze, modify, and enhance signals that are free from aliasing or modulatory effects, the literature presently lacks a unified filterbank theory for these settings.

In this work we develop a set of results necessary to fully understand and exploit the *local* aliasing and modulation properties of sampled signals and their subband representations. Though our motivation stems from signal processing problems typically encountered in practice (such as those mentioned above, to which we return at the end of the article), our results are more general, showing equivalences between certain "rewirings" of filterbank block diagrams, and the corresponding actions of convolution, modulation, and downsampling operators. Our primary contributions are the introduction and analysis of two cardinal rewiring mechanisms—reverse-order subband structure (ROSS) and subband convolution structure (SCS)—by which filterbank subbands are coupled together to describe the relationship between localized aliasing, modulation, and convolution.

The framework we introduce is distinct from work involving signal recovery methods [3]–[8] and sampling theorems [9]–[12] in the extant literature. Such work has successfully characterized sufficient conditions for exact reconstruction when filterbank theory is used to restrict the class of signals under consideration, or to specify the fundamental compressibility of

(a) x (b) x_m (c) x_s

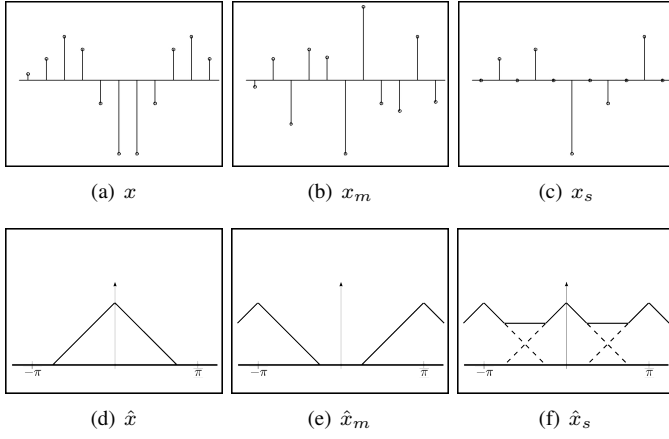(d) $\hat{x}$ (e) $\hat{x}_m$ (f) $\hat{x}_s$

Fig. 1. Pictorial illustrations of modulation and sampling in both the time (a-c) and frequency (d-f) domains.

its members. In contrast, this article employs filterbank theory to describe the data acquisition and sampling process itself, rather than any properties of a given signal class. Notions of localized aliasing and localized modulation are intimately connected with the ROSS and SCS analyses that we introduce below, and are also complementary to other well-understood concepts in filterbank analysis.

The article is organized as follows. In the remainder of Section I we introduce key definitions and filterbank notation, and provide a simple example of local aliasing and local modulation that motivates our subsequent analysis. In Section II we introduce our first "rewiring" notion—that of reverse-order subband structure—and derive corresponding expressions for the filterbank coefficients corresponding to a subsampled signal. In Section III we build on this work to introduce the notion of subband convolution structure— our second means of filterbank rewiring—and show how it leads to a convolution theorem particularly suited to the local modularity of the filterbank transform. We conclude with a discussion in Section IV where we consider the practical use of these two notions in problems involving missing data, multiplexed signal acquisition, and signal-dependent noise.

A. Key Definitions and Filterbank Notation

Throughout, let $x \in \ell^2(\mathbb{Z})$ be a real-valued sequence indexed by $n \in \mathbb{Z}$. *Subsampling* is the operation of replacing every odd-numbered element of x by zero, and hence the *subsampled sequence* x_s is defined element-wise as

$$x_s[n] := \begin{cases} x[n] & \text{if } n \text{ even,} \\ 0 & \text{if } n \text{ odd.} \end{cases}$$

(Note that this is distinct from *downsampling*, a dilation of the index set of x to yield $x[2n]$, such that odd-numbered samples are "dropped" and only even-numbered ones retained.) Equivalently, $x_s[n]$ is an arithmetic average of $x[n]$ and its frequency-*modulated* version $x_m[n] := (-1)^n x[n]$.:

$$x_s[n] = \frac{1}{2}\left(x[n] + x_m[n]\right).$$

(a) One-level filterbank structure
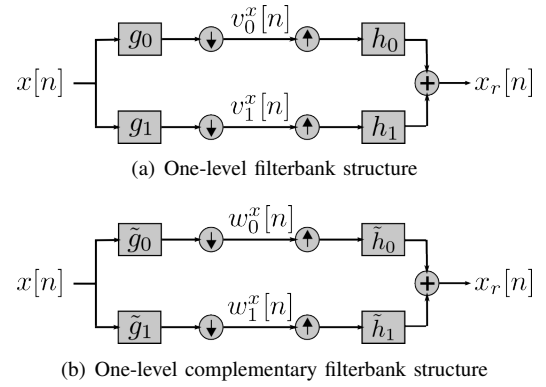
(b) One-level complementary filterbank structure

Fig. 2. One-level filterbank (a) and its complementary structure (b). Diagram (a) represents analysis and synthesis filters $\{g_0, g_1\}$ and $\{h_0, h_1\}$, respectively, as well as filterbank coefficient sets $\{v_0^x, v_1^x\}$ resulting from the action of the analysis convolution operator and subsequent downsampling on a sequence x. Reversing the downsampling procedure and applying the synthesis filters yields a "reconstructed" sequence x_r. Diagram (b) represents filters $\tilde{g}_i, \tilde{h}_i$ "complementary" to (a), obtained by swapping the roles of g and h, respectively, and then applying an affine transformation.

Figures 1(a)-(c) serve as a reminder to illustrate how samples in x and x_m with opposite signs cancel out to yield x_s; we shall frequently refer back to them later.

Let $\hat{x}$ denote the discrete-time Fourier transform of x, with $\omega \in \mathbb{R}/2\pi$ its corresponding normalized angular frequency. Then it follows that $\hat{x}_m(\omega) = \hat{x}(\omega - \pi)$ and

$$\hat{x}_s(\omega) = \frac{1}{2}\left[\hat{x}(\omega) + \hat{x}(\omega - \pi)\right]. \tag{1}$$

Here we see that when the bandwidth of x—i.e., the support of $\hat{x}$—is sufficiently large, $\hat{x}(\omega)$ and $\hat{x}_m(\omega)$ are indistinguishable in $\hat{x}_s(\omega)$; as shown in Figures 1(d)-(g), their supports overlap in the Fourier domain. This phenomenon is called *aliasing*; in the absence of additional information, aliased portions of x cannot be recovered from $\hat{x}_s(\omega)$ alone.

The Fourier transform is a fundamentally global operation; modulation and aliasing mix non-local information from the sequence x. In contrast, a *filterbank* maps a sequence x to some alternative representation by way of localized *filterbank coefficients* ("analysis"), and subsequently yields a linear reconstruction x_r ("synthesis"); well-known examples include short-time Fourier and wavelet representations. As the analysis operator acts linearly, we write its action as an inner product, calling it a filter when it is a convolution operator parameterized by translation along a sublattice of $\mathbb{Z}$, as is the case considered here. If this convolution operator is represented by the actions of a finite-length, real-valued sequences in $\ell^2(\mathbb{Z})$, then we refer to a real-valued, finite-impulse-response analysis filter g and corresponding synthesis filter h. Figure 2(a) illustrates a basic filterbank structure, with two analysis filters $\{g_0, g_1\}$ and two synthesis filters $\{h_0, h_1\}$. We denote by $\{v_0^x, v_1^x\}$ the corresponding filterbank coefficient sequences, defined as follows.

Definition 1.1 (Filterbank Coefficient Sequence): We call $v_i^x \in \ell^2(\mathbb{Z})$ a one-level filterbank coefficient sequence corresponding to x if

$$v_i^x[n] := \left(g_i[m] \star_m x[m]\right)[2n], \tag{2}$$

where the summation in the discrete convolution $\star_m$ is performed over the index m, and the subsequent notion of downsampling by two is reflected by the index set $\{2n : n \in \mathbb{Z}\}$.

This composition of convolution and dilation implies in turn that

$$\hat{v}_i^x(\omega) = \frac{1}{2}\left[\hat{g}_i\left(\frac{\omega}{2}\right)\hat{x}\left(\frac{\omega}{2}\right) + \hat{g}_i\left(\frac{\omega}{2} - \pi\right)\hat{x}\left(\frac{\omega}{2} - \pi\right)\right],\tag{3}$$

and the set of transform coefficients $\{v_i^x[n]\}_{n\in\mathbb{Z}}$ is collectively referred to as the ith filterbank subband. Typically g_0 and h_0 are smooth (i.e., low-pass) filters, while g_1 and h_1 have zero average. Thus, v_0^x provides a measure of local low-frequency energy concentration, while v_1^x captures local high-frequency energy, with temporal localization provided by the finite support of $\{g_i, h_i\}_{i\in\mathbb{Z}_2}$. A filterbank's joint time-frequency resolution can be fine-tuned by recursively nesting copies of the basic one-level transform structure illustrated in Figure 2(a), yielding the multi-level filterbank structures that we consider later in Section II-C.

Note that the Fourier representation of (3) implies the superposition of shifted copies of the resultant filtered spectra, which in general will give rise to aliasing of the type illustrated in Figure 1(f). It is thus natural to ask for conditions under which this aliasing will cancel—a prerequisite for the exact reconstruction of any input sequence $x \in \ell^2(\mathbb{Z})$ from its filterbank coefficients, such that $x_r = x$ in the diagram of Figure 2(a). To this end we arrive at the following well-known definition, which stems from *global* properties of the Fourier transform.

Definition 1.2 (Perfect Reconstruction Filterbank): A *perfect reconstruction filterbank* $\{g_i, h_i\}_{i\in\mathbb{Z}_2}$ admits for all $x \in \ell^2(\mathbb{Z})$ the relation

$$\hat{x}_{(\omega)} := \hat{h}_0(\omega)\hat{v}_0^x(2\omega) + \hat{h}_1(\omega)\hat{v}_1^x(2\omega) = \hat{x}(\omega).\tag{4}$$

Equivalently, as shown in Figure 2(a), we have for all $n \in \mathbb{Z}$ that

$$\begin{aligned}x_r[2n] =& \Big(h_0[2m] \star_m v_0^x[m]\Big)[n]\\&+ \Big(h_1[2m] \star_m v_1^x[m]\Big)[n] = x[2n]\\x_r[2n+1] =& \Big(h_0[2m+1] \star_m v_0^x[m]\Big)[n]\\&+ \Big(h_1[2m+1] \star_m v_1^x[m]\Big)[n] = x[2n+1].\end{aligned}$$

As described earlier, the sequences of operations corresponding to the forward transform step in (2) and the reconstruction step in (4) are commonly referred to as the *analysis* and *synthesis filterbanks*, respectively.

Remark 1.1 (Haar Filterbank Transform): Perhaps the most well-known example of a perfect reconstruction filterbank is given by the so-called Haar transform, which may be defined in terms of its z-transform as:

$$\begin{aligned}\sum_n g_i[n]z^{-n} =& 1 + (-1)^i z,\\\sum_n h_i[n]z^{-n} =& \frac{1}{2}\left[(-1)^i + z^{-1}\right].\end{aligned}\tag{5}$$

Note that g_0 and g_1 in (5) amount to the sum and difference of neighboring samples, respectively, and it is clear that the original sequence $x[n]$ is easily recoverable from the corresponding sequences of filterbank coefficients.

Important and well-known results associated with Definition 1.2 established the following (see, e.g., [1]) .

Property 1.1 (Alias Cancellation Equivalence): The set $\{g_i, h_i\}_{i\in\mathbb{Z}_2}$ is a perfect reconstruction filterbank if and only if

$$2 = \hat{g}_0(\omega)\hat{h}_0(\omega) + \hat{g}_1(\omega)\hat{h}_1(\omega)\tag{6}$$
$$0 = \hat{g}_0(\omega)\hat{h}_0(\omega - \pi) + \hat{g}_1(\omega)\hat{h}_1(\omega - \pi)\tag{7}$$

Property 1.2 (Analysis-Synthesis Symmetry): If finite-impulse-response filters $\{g_i, h_i\}_{i\in\mathbb{Z}_2}$ comprise a perfect reconstruction filterbank, then there exist $a \in \mathbb{R} \setminus \{0\}$ and $b \in \mathbb{Z}$ such that

$$\hat{g}_i(\omega) = (-1)^{1-i}ae^{j(2b+1)\omega}\hat{h}_{1-i}(\omega - \pi).$$

Remark 1.2: The condition of (7) in Property 1.1 guarantees that the aliased components in v_0^x and v_1^x cancel, so the impulse response of the overall filterbank structure in Figure 2(a) is equal to one-half of the expression of (6); i.e., everywhere constant and equal to unity. Property 1.2 makes explicit the fact that an analysis filterbank uniquely defines its corresponding synthesis filterbank. These properties serve as the foundation for the reverse-order subband filterbank structure that we introduce in Section II below.

B. Motivating Example for Filterbank "Rewiring"

The preceding section has served to introduce the basic notions of filterbank theory that we shall employ here. Before continuing, it is instructive to consider a simple motivating example based on the simplest case of the Haar filterbank transform. In essence, we will see that "rewiring" filterbank diagrams such as those in Figure 3 can be related to the actions of convolution, modulation, and downsampling operators. In subsequent sections we develop these properties formally, and show how they yield new insights into important practical problems.

To begin, consider the symmetric Hadamard matrix

$$\mathbf{\Phi} = \begin{bmatrix} 1 & 1 \\ 1 & -1 \end{bmatrix}$$

which maps two-dimensional vectors to the corresponding sums and difference of their components, and thus serves to define the (unnormalized) one-level Haar filterbank. Note that $\mathbf{\Phi}^{-1} = \frac{1}{2}\mathbf{\Phi}$, and consider two systems of linear equations in $\mathbf{\Phi}$ that will serve to illustrate the concepts of reverse-order and convolution subband structure:

$$\begin{bmatrix} q \\ r \end{bmatrix} = \mathbf{\Phi}\begin{bmatrix} a \\ b \end{bmatrix}, \qquad \begin{bmatrix} s \\ t \end{bmatrix} = \mathbf{\Phi}\begin{bmatrix} c \\ d \end{bmatrix}.$$

Example 1.1 (Reverse-Ordering and Subsampling):
Consider the first system of equations above, and suppose that we replace b with $-b$, yielding a "modulated" version of $[a, b]^T$. We then observe that the Haar transform of $[a, -b]^T$ results in a *reverse-ordering* of q and r, which play the roles

of low-pass and high-pass components, respectively:

$$\begin{bmatrix} 1 & 1 \\ 1 & -1 \end{bmatrix} \begin{bmatrix} a \\ -b \end{bmatrix} = \frac{1}{2} \begin{bmatrix} 1 & 1 \\ 1 & -1 \end{bmatrix} \begin{bmatrix} 1 & 1 \\ -1 & 1 \end{bmatrix} \begin{bmatrix} q \\ r \end{bmatrix} = \begin{bmatrix} r \\ q \end{bmatrix}.$$

Since summing $[a,b]^T$ and its modulated version corresponds to subsampling, we next compute the Haar transform of $[a,0]^T$, and observe that this results in an arithmetic averaging of q and r:

$$\begin{bmatrix} 1 & 1 \\ 1 & -1 \end{bmatrix} \begin{bmatrix} a \\ 0 \end{bmatrix} = \frac{1}{2} \begin{bmatrix} 1 & 1 \\ 1 & -1 \end{bmatrix} \left(\begin{bmatrix} a \\ b \end{bmatrix} + \begin{bmatrix} a \\ -b \end{bmatrix} \right) = \frac{1}{2} \begin{bmatrix} q+r \\ q+r \end{bmatrix}.$$

We see from this simple example that the "swapping" and the "combining" of *low-pass* and *high-pass* components are reminiscent of modulation and aliasing in the traditional Fourier sense, as illustrated respectively in Figures 1(e) and 1(f).

Example 1.2 (Convolution and Pointwise Multiplication): Now consider the element-wise product of the vectors $[a,b]^T$ and $[c,d]^T$. The Haar transform of this product $[ac,bd]^T$ is:

$$\begin{aligned} \begin{bmatrix} 1 & 1 \\ 1 & -1 \end{bmatrix} \begin{bmatrix} ac \\ bd \end{bmatrix} &= \frac{1}{4} \begin{bmatrix} 1 & 1 \\ 1 & -1 \end{bmatrix} \begin{bmatrix} (q+r)(s+t) \\ (q-r)(s-t) \end{bmatrix} \\ &= \frac{1}{4} \begin{bmatrix} (q+r)(s+t) + (q-r)(s-t) \\ (q+r)(s+t) - (q-r)(s-t) \end{bmatrix} \\ &= \frac{1}{2} \begin{bmatrix} qs+rt \\ qt+sr \end{bmatrix}. \end{aligned}$$

The symmetry of $qs+rt$ and $qt+sr$ suggests a kind of cyclic convolution of $[q,r]^T$ and $[s,t]^T$. In fact, we will see in Section III that our filterbank rewiring techniques recover precisely this notion of group structure, in direct analogy to *global* Fourier analysis. In Section IV, these ideas will reappear in the context of analysis of signals subject to multiplicative noise corruption.

II. REVERSE-ORDER SUBBAND STRUCTURE AND LOCALIZED ALIASING

Having introduced the necessary definitions and given two brief examples, we now begin our technical development of filterbank "rewiring." Bearing in mind the examples considered above, we introduce in Section II-A below the notion of *complementary filterbanks*, and then employ them to obtain the following results in Section II-B: the *reverse-ordering of subband structure* that results from modulation, and *localized aliasing* that stems from averaging the low- and high-frequency filterbank coefficients. In Section II-C we extend these results to the setting of multi-level filterbanks.

A. Complementary Filterbanks

Definition 2.1: (Complementary Filterbanks and Filterbank Coefficients): Let $\{g_i, h_i\}_{i \in \mathbb{Z}_2}$ be a perfect reconstruction filterbank. Then we define the *complementary filterbank* $\{\tilde{g}_i, \tilde{h}_i\}_{i \in \mathbb{Z}_2}$ as follows:

$$\begin{aligned} \tilde{g}_i[n] &:= ah_i[n + (2b+1)] \\ \tilde{h}_i[n] &:= a^{-1}g_i[n - (2b+1)], \end{aligned}$$

where a and b are chosen to satisfy Property 1.2 of perfect reconstruction filterbank, and we call $w_i^x[n]$ a one-level *complementary filterbank coefficient* corresponding to a sequence

x if

$$w_i^x[n] := \Big(\tilde{g}_i[m] \star_m x[m]\Big)[2n].$$

The following important property of complementary filterbanks follows directly from Properties 1.1 and 1.2 of perfect reconstruction filterbanks.

Proposition 2.1 (Complementarity & Perfect Reconstruction): If the set $\{g_i, h_i\}_{i \in \mathbb{Z}_2}$ is a perfect reconstruction filterbank, then so is $\{\tilde{g}_i, \tilde{h}_i\}_{i \in \mathbb{Z}_2}$.

Proof: Appealing to Property 1.2, we see that Fourier transforms of $\tilde{g}_i$ and $\tilde{h}_i$ respectively yield

$$\begin{aligned} \hat{\tilde{g}}_i(\omega) &= ae^{j(2b+1)\omega}\hat{h}_i(\omega) \\ \hat{\tilde{h}}_i(\omega) &= a^{-1}e^{-j(2b+1)\omega}\hat{g}_i(\omega). \end{aligned} \tag{8}$$

By substitution, we verify that (6) and (7) hold for $\{\tilde{g}_i, \tilde{h}_i\}_{i \in \mathbb{Z}_2}$:

$$\begin{aligned} &\hat{\tilde{g}}_0(\omega)\hat{\tilde{h}}_0(\omega) + \hat{\tilde{g}}_1(\omega)\hat{\tilde{h}}_1(\omega) \\ &= \Big(ae^{j(2b+1)\omega}\hat{h}_0(\omega)\Big)\Big(a^{-1}e^{-j(2b+1)}\hat{g}_0(\omega)\Big) \\ &\quad + \Big(ae^{j(2b+1)\omega}\hat{h}_1(\omega)\Big)\Big(a^{-1}e^{-j(2b+1)}\hat{g}_1(\omega)\Big) = 2 \\ &\hat{\tilde{g}}_0(\omega)\hat{\tilde{h}}_0(\omega - \pi) + \hat{\tilde{g}}_1(\omega)\hat{\tilde{h}}_1(\omega - \pi) \\ &= \Big(ae^{j(2b+1)\omega}\hat{h}_0(\omega)\Big)\Big(a^{-1}e^{-j(2b+1)}\hat{g}_0(\omega - \pi)\Big) \\ &\quad + \Big(ae^{j(2b+1)\omega}\hat{h}_1(\omega)\Big)\Big(a^{-1}e^{-j(2b+1)}\hat{g}_1(\omega - \pi)\Big) = 0. \end{aligned}$$

Hence by Property 1.1, the set $\{\tilde{g}_i, \tilde{h}_i\}_{i \in \mathbb{Z}_2}$ comprises a perfect reconstruction filterbank. ∎

Figure 2(b) illustrates this complementary filterbank structure, along with the corresponding complementary coefficients w_i^x. It is natural to ask if a filterbank can be its own complement, and to this end we have the following.

Definition 2.2 (Self-Complementary Filterbank): We call a filterbank $\{g_i, h_i\}_{i \in \mathbb{Z}_2}$ *self-complementary* if

$$v_i^x[n] = (-1)^{1-i}w_i^x[n]. \tag{9}$$

Returning now to Remark 1.1, we note the following.

Proposition 2.2 (Self-Complementarity of Haar Filterbank): The Haar filterbank is self-complementary.

Proof: It follows from (5) that the Haar filterbank satisfies the following symmetry:

$$\hat{g}_i(\omega) = (-1)^i e^{j(2b+1)\omega}\hat{g}_i^*(\omega),$$

with $a = \frac{1}{2}$ and $b = -1$. Applying Property 1.2 of perfect reconstruction filterbanks in turn yields

$$\begin{aligned} (-1)^i e^{j(2b+1)\omega}\hat{g}_i^*(\omega) &= (-1)^{1-i}ae^{j(2b+1)\omega}\hat{h}_{1-i}(\omega - \pi) \\ \hat{g}_i^*(\omega) &= -a\hat{h}_{1-i}(\omega - \pi). \end{aligned} \tag{10}$$

The well-known identity $\hat{g}_i(\omega) = (-1)^i e^{j(2b+1)\omega}\hat{g}_{1-i}^*(\omega - \pi)$ of Smith and Barnwell [13] applies; and upon substituting this into (10), we obtain the desired result:

$$\begin{aligned} \hat{g}_i(\omega) &= (-1)^i e^{j(2b+1)\omega}(-a\hat{h}_i(\omega)) \\ &= (-1)^{1-i}\hat{\tilde{g}}_i(\omega). \end{aligned}$$
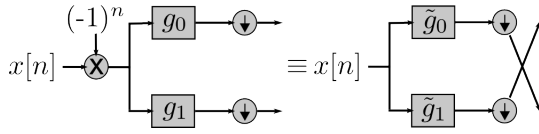
∎

Fig. 3. Illustration of Theorem 1, with the left side showing a modulated signal $x_m[n]$ and the right side showing reverse-ordering of the complementary filterbank. The low- and high-frequency filterbank subbands for the modulated signal behave like the high- and low-frequency complementary filterbank subbands for the original signal, respectively.

As we show below, complementary filterbanks play a key role in the reverse-ordering of subband structure induced by modulation.

B. Reverse-Order Subband Structure

Figure 3 illustrates the *reversal of subband ordering* that results when x is modulated by π to yield x_m: the low-frequency filterbank coefficient for the modulated signal ($v_0^{x_m}[n]$) behaves like the high-frequency complementary filterbank coefficient for the original signal ($w_1^x[n]$), and vice-versa. As may be seen by comparing Figure 3 with Figure 1, this filterbank subband "role-reversal" is consistent with the Fourier interpretation of modulation by π; in both cases, the low- and high-frequency components are swapped, modulo-2π. We formalize this notion as follows:

Theorem 1 (Reverse-Order Subband Structure (ROSS)): If the set $\{g_i, h_i\}_{i \in \mathbb{Z}_2}$ is a perfect reconstruction filterbank, then

$$v_i^{x_m}[n] = (-1)^i w_{1-i}^x[n]. \tag{11}$$

Proof: Modulation of x by π implies that we have that

$$\hat{v}_i^{x_m}(\omega) = \frac{1}{2}\left[\hat{g}_i\left(\frac{\omega}{2}\right)\hat{x}_m\left(\frac{\omega}{2}\right) + \hat{g}_i\left(\frac{\omega}{2} - \pi\right)\hat{x}_m\left(\frac{\omega}{2} - \pi\right)\right]$$
$$= \frac{1}{2}\left[\hat{g}_i\left(\frac{\omega}{2}\right)\hat{x}\left(\frac{\omega}{2} - \pi\right) + \hat{g}_i\left(\frac{\omega}{2} - \pi\right)\hat{x}\left(\frac{\omega}{2}\right)\right].$$

By Property 1.2 of perfect reconstruction filterbanks and Definition 2.1,

$$\hat{g}_i(\omega) = (-1)^{1-i} a e^{j(2b+1)\omega}\hat{h}_{1-i}(\omega - \pi)$$
$$= (-1)^i \hat{\tilde{g}}_{1-i}(\omega - \pi)$$
$$\hat{v}_i^{x_m}(\omega)$$
$$= \frac{(-1)^i}{2}\left[\hat{\tilde{g}}_{1-i}\left(\frac{\omega}{2}\right)\hat{x}\left(\frac{\omega}{2}\right) + \hat{\tilde{g}}_{1-i}\left(\frac{\omega}{2} - \pi\right)\hat{x}\left(\frac{\omega}{2} - \pi\right)\right]$$
$$= (-1)^i \hat{w}_{1-i}^x(\omega). \tag{12}$$
∎

Applying Property 1.1 of perfect reconstruction filterbanks to (12) immediately yields the following important corollary.

Corollary 2.1 (Modulation induced by ROSS): Suppose the set $\{g_i, h_i\}_{i \in \mathbb{Z}_2}$ is a perfect reconstruction filterbank. Then

$$0 = \hat{\tilde{g}}_1(\omega)\hat{h}_0(\omega) - \hat{\tilde{g}}_0(\omega)\hat{h}_1(\omega),$$
$$2 = \hat{\tilde{g}}_1(\omega)\hat{h}_0(\omega - \pi) - \hat{\tilde{g}}_0(\omega)\hat{h}_1(\omega - \pi).$$

Remark 2.1 (Filterbank Interpretation of ROSS Modulation): An intuitive interpretation of Corollary 2.1 is that exchanging the low- and high-frequency filterbank subbands results in modulation. To see this, consider reconstruction of the
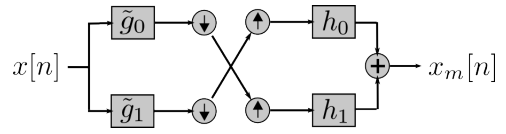

Fig. 4. Illustration of Corollary 2.1: exchange of low- and high-frequency filterbank subbands results in modulation (compare to the standard complementary filterbank structure of Figure 2(b)).
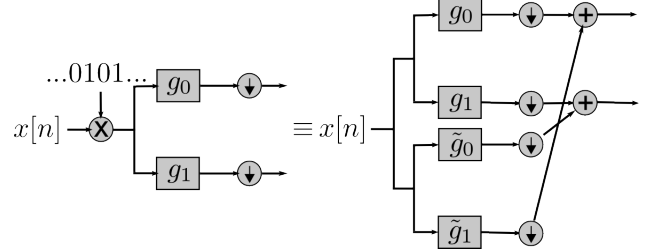

Fig. 5. Illustration of Corollary 2.2, with the left side showing $x[n]$ subject to subsampling and the right side showing the corresponding aliasing structure. Filterbank coefficients corresponding to the subsampled signal are arithmetic averages of *complementary* low- and high-frequency coefficients.

complementary filterbank coefficients with *reverse-order* subbands, as illustrated in Figure 4:

$$\hat{x}_r(\omega) = \hat{h}_0(\omega)\hat{w}_1^x(2\omega) - \hat{h}_1(\omega)\hat{w}_0^x(2\omega)$$
$$= \frac{1}{2}\hat{h}_0(\omega)\left[\hat{\tilde{g}}_1(\omega)\hat{x}(\omega) + \hat{\tilde{g}}_1(\omega - \pi)\hat{x}(\omega - \pi)\right]$$
$$\quad - \frac{1}{2}\hat{h}_1(\omega)\left[\hat{\tilde{g}}_0(\omega)\hat{x}(\omega) + \hat{\tilde{g}}_0(\omega - \pi)\hat{x}(\omega - \pi)\right]$$
$$= \frac{1}{2}\hat{x}(\omega)\left[\hat{h}_0(\omega)\hat{\tilde{g}}_1(\omega) - \hat{h}_1(\omega)\hat{\tilde{g}}_0(\omega)\right]$$
$$\quad + \frac{1}{2}\hat{x}(\omega - \pi)\left[\hat{h}_0(\omega)\hat{\tilde{g}}_1(\omega - \pi) - \hat{h}_1(\omega)\hat{\tilde{g}}_0(\omega - \pi)\right]$$
$$= \hat{x}(\omega - \pi).$$

We also obtain a filterbank interpretation of the *aliasing induced by subsampling*, in analogy to the Fourier decomposition of (1). As shown in Figure 5, filterbank coefficients corresponding to the subsampled signal $x_s[n]$ are arithmetic averages of low- and high-frequency coefficients corresponding to $x[n]$, in analogy to the symmetry about $\pi/2$ visible in the Figure 1(f).

Corollary 2.2 (Localized Aliasing): If the set $\{g_i, h_i\}_{i \in \mathbb{Z}_2}$ is a perfect reconstruction filterbank, then by linearity and Theorem 1,

$$v_i^{x_s}[n] = \frac{1}{2}\left(v_i^x[n] + (-1)^i w_{1-i}^x[n]\right).$$

Furthermore, this modulation implies the filterbank subband symmetry $v_i^{x_s}[n] = (-1)^i w_{1-i}^{x_s}[n]$.

As can be seen in Figure 5, *localized aliasing* occurs when $v_i^x[n]$ and $w_{1-i}^x[n]$ are both simultaneously nonzero and hence indistinguishable in $v_i^{x_s}[n]$. Unlike the global Fourier aliasing illustrated in Figure 1, however, this aliasing is confined to a temporally localized region that depends on the local regularity of x.

C. Extension to Multi-Level Setting

Multi-level filterbank analysis corresponds to a recursive application of convolution and downsampling operators to successive sets of filterbank coefficients. To index the corresponding subbands, we adopt *binary* vector notation for indices as follows. Let $\boldsymbol{i} = (i_{I\text{-}1}, \ldots, i_1, i_0)^T \in \mathbb{Z}_2{}^I$ and $\boldsymbol{i}' = (i_{I\text{-}1}, \ldots, i_1, 1 - i_0)^T$, and recalling $v_{\boldsymbol{i}}^x[n]$ and $w_{\boldsymbol{i}}^x[n]$ from Definitions 1.1 and 2.1, define the corresponding I-level recursions:

$$v_{\boldsymbol{i}}^x[n] := \Big(g_{i_{I\text{-}1}} \star_{m_{I\text{-}1}} \Big(\ldots \Big(g_{i_1}[m_1] \star_{m_1} \Big(g_{i_0}[m_0] \\ \star_{m_0} x[m_0] \Big)[2m_1] \Big)[2m_2] \ldots \Big)[2m_{I\text{-}1}] \Big)[2n] \tag{13}$$

$$w_{\boldsymbol{i}}^x[n] := \Big(g_{i_{I\text{-}1}} \star_{m_{I\text{-}1}} \Big(\ldots \Big(g_{i_1}[m_1] \star_{m_1} \Big(\tilde{g}_{i_0}[m_0] \\ \star_{m_0} x[m_0] \Big)[2m_1] \Big)[2m_2] \ldots \Big)[2m_{I\text{-}1}] \Big)[2n]. \tag{14}$$

Here $i_k \in \mathbb{Z}_2$ indexes the analysis filters used in the kth-level decomposition (i.e. g_0 or g_1), and $\boldsymbol{i}'$ corresponds to a high (low) frequency subband when $\boldsymbol{i}$ is a low (high) frequency subband. Note here that the *complementary* filters $\tilde{g}_0$ and $\tilde{g}_1$ are used *only* in the 0th-level decomposition in (14). The corresponding perfect reconstruction extension of (4) to the case of an I-level filterbank is

$$\hat{x}_r(\omega) := \sum_{\boldsymbol{i}} \hat{v}_{\boldsymbol{i}}^x(2^I \omega) \prod_{k=0}^{I-1} \hat{h}_{i_k}(2^k \omega). \tag{15}$$

Then, in parallel to our earlier development, the results of Theorem 1 and Corollary 2.2 extend to the multi-level setting as follows.

Theorem 2 (Multi-Level ROSS): Suppose the set $\{g_i, h_i\}_{i \in \mathbb{Z}_2}$ is a perfect reconstruction filterbank, and let $\boldsymbol{i} \in \mathbb{Z}_2{}^I$. Then,

$$v_{\boldsymbol{i}}^{x_m} = (-1)^{i_0} w_{\boldsymbol{i}'}^x[n];$$
$$v_{\boldsymbol{i}}^{x_s} = (-1)^{i_0} w_{\boldsymbol{i}'}^{x_s}[n] = \frac{1}{2}\Big(v_{\boldsymbol{i}}^x[n] + (-1)^{i_0} w_{\boldsymbol{i}'}^x[n] \Big).$$

Using the same example shown in Figure 1, Figure 6 illustrates this localized aliasing in the multi-level filterbank setting. Note that although the subsampled example signal is subject to aliasing in a global sense (Figure 1(f)), the corresponding $v_{\boldsymbol{i}}^x[n]$ may be recovered from $v_{\boldsymbol{i}}^{x_s}[n]$ whenever $w_{\boldsymbol{i}'}^x[n] = 0$. Theorem 2 simplifies when self-complimentarity is taken into account, illustrated also in Figure 7.

Corollary 2.3 (Multi-Level Self-Complementary ROSS): If the set $\{g_i, h_i\}_{i \in \mathbb{Z}_2}$ is a perfect reconstruction filterbank that is also self-complementary, then

$$v_{\boldsymbol{i}}^x[n] = (-1)^{1-i_0} w_{\boldsymbol{i}}^x[n],$$
$$v_{\boldsymbol{i}}^{x_m}[n] = v_{\boldsymbol{i}'}^x[n];$$
$$v_{\boldsymbol{i}}^{x_s}[n] = \frac{1}{2}\Big(v_{\boldsymbol{i}}^x[n] + v_{\boldsymbol{i}}^{x_m}[n] \Big) = \frac{1}{2}\Big(v_{\boldsymbol{i}}^x[n] + v_{\boldsymbol{i}'}^x[n] \Big).$$

Remark 2.2 (Extension to Discrete Wavelet Transform): The above results can easily be adapted to discrete wavelet transforms, which employ the same fundamental building blocks as perfect reconstruction filterbanks [1], [2]. As an example, the filterbank rewiring associated with the wavelet transform of a subsampled signal $x_s[n]$ is illustrated in Figure 8; we leave the details as an easy exercise for the reader.

(a) $v_{\boldsymbol{i}}^x$ (b) $v_{\boldsymbol{i}}^{x_m}$ (c) $v_{\boldsymbol{i}}^{x_s}$ (d) $w_{\boldsymbol{i}}^x$
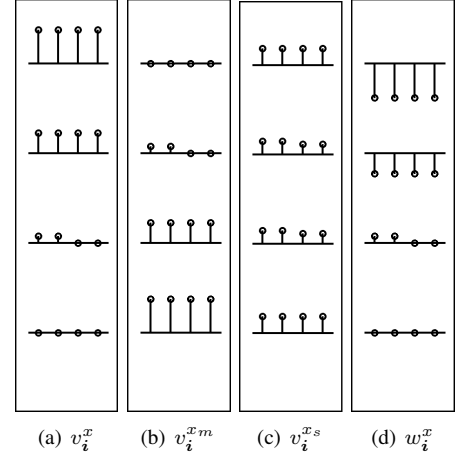
Fig. 6. Pictorial illustration of *localized aliasing* in the 2-level filterbank domain, as indicated by Theorem 2. Parts (a-c) show filterbank coefficients sequences corresponding to Fig. 1(a-c), respectively, with (d) the complementary sequence corresponding to Fig. 1(a). From top to bottom, the ordering of the four subbands represented in each subfigure is $\boldsymbol{i} = (0,0), (1,0), (1,1), (0,1)$. "Rewiring" is evident in comparing (b) with (d), and $v_{\boldsymbol{i}}^x[n]$ is exactly recoverable from $v_{\boldsymbol{i}}^{x_s}[n]$ whenever $w_{\boldsymbol{i}'}^x[n] = 0$.

III. SUBBAND CONVOLUTION STRUCTURE AND LOCALIZED MODULATION

In the previous section, we introduced and studied the reverse-ordering of subband structure induced by subsampling, for the case of general perfect reconstruction filterbanks. Furthermore, we saw that this structure simplified considerably when self-complimentarity was taken into account. In this section, we show that the symmetry of the Haar filterbank transform also affords a characterization of Fourier group duality and convolution. As a special case, we recover the multi-level ROSS structure of Corollary 2.3, thereby linking the ROSS results of Section II and the subband convolution structure (SCS) we introduce below.

A. Subband Convolution Structure

Recall the multi-level filterbank decomposition of (13), in which $i_k \in \mathbb{Z}_2$ indexes pairs of analysis filters used for the kth level decomposition. Below, we prove the duality of time-domain multiplication and *subband convolution* of filterbank coefficients in this context.

Theorem 3 (Subband Convolution): Let $v_{\boldsymbol{i}}^x, v_{\boldsymbol{i}}^y$ be I-level Haar filterbank coefficient sequences corresponding to x and y, respectively, with $v_{\boldsymbol{i}}^{xy}[n]$ that of the element-wise product xy. Then, letting $\circledast$ denote cyclic convolution, we have the relation

$$\Big(v_{\boldsymbol{j}}^x \circledast_{\boldsymbol{j}} v_{\boldsymbol{j}}^y \Big)_{\boldsymbol{i}}[n] := \frac{1}{2^I} \sum_{\boldsymbol{j}} v_{\boldsymbol{i}+\boldsymbol{j}}^x[n] v_{\boldsymbol{j}}^y[n] = v_{\boldsymbol{i}}^{xy}[n].$$
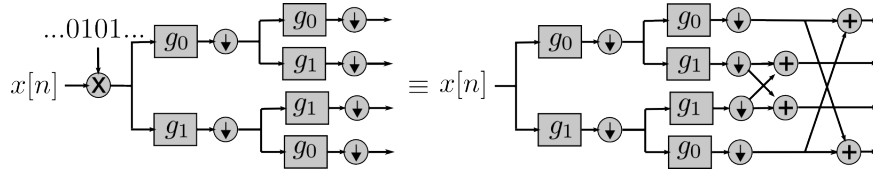
Fig. 7. Illustration of Corollary 2.3. Filterbank coefficients corresponding to the subsampled signal are arithmetic averages of reverse-order coefficients. *Localized aliasing* thus occurs when $v_{\boldsymbol{i}}^x[n]$ and $w_{\boldsymbol{i}'}^x[n]$ are both supported simultaneously and hence indistinguishable in $v_{\boldsymbol{i}}^{x_s}[n]$.
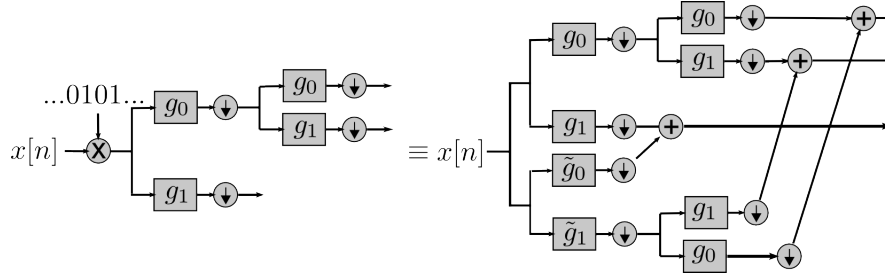

Fig. 8. An example of ROSS-based *wavelet* analysis, with the left side showing $x[n]$ subject to subsampling, and the right side showing the corresponding aliasing structure.

Proof: By the Fourier representation of (15), the product $x[n] \cdot y[n]$ can be analyzed as:

$$\widehat{(x \cdot y)}(\omega) = \hat{x}_r(\omega) \star_\omega \hat{y}_r(\omega)$$

$$= \left[\sum_{\boldsymbol{i}} \hat{v}_{\boldsymbol{i}}^x(2^I \omega) \prod_{k=0}^{I-1} \hat{h}_{i_k}(2^k \omega) \right] \star_\omega \left[\sum_{\boldsymbol{j}} \hat{v}_{\boldsymbol{j}}^x(2^I \omega) \prod_{k=0}^{I-1} \hat{h}_{j_k}(2^k \omega) \right]$$

$$= \sum_{\boldsymbol{i}} \sum_{\boldsymbol{j}} \int_{-\pi}^{\pi} \hat{v}_{\boldsymbol{i}}^x(2^I \nu) \hat{v}_{\boldsymbol{j}}^x \left(2^I (\omega - \nu) \right)$$

$$\cdot \left[\prod_{k=0}^{I-1} \hat{h}_{i_k}(2^k \nu) \hat{h}_{j_k} \left(2^k (\omega - \nu) \right) \right] d\nu. \tag{16}$$

It follows from the definition of the Haar filterbank transform in (5) that

$$\hat{h}_{i_k}(2^k \nu) \hat{h}_{j_k} \left(2^k (\omega - \nu) \right)$$

$$= \frac{1}{4} \left[(-1)^{i_k} + e^{-j2^k \nu} \right] \left[(-1)^{j_k} + e^{-j2^k(\omega-\nu)} \right]$$

$$= \frac{1}{2} \left[\hat{h}_{i_k+j_k}(2^k \omega) + (-1)^{i_k} e^{-j2^k \nu} \hat{h}_{i_k+j_k} \left(2^k (\omega - 2\nu) \right) \right].$$

Substituting this expression into (16) for $k = 0$,

$$\widehat{(x \cdot y)}(\omega) = \frac{1}{2} \sum_{\boldsymbol{i}} \sum_{\boldsymbol{j}} \int_{-\pi}^{\pi} \hat{v}_{\boldsymbol{i}}^x(2^I \nu) \hat{v}_{\boldsymbol{j}}^x$$

$$\cdot \left(2^I (\omega - \nu) \right) \left[\prod_{k=1}^{I-1} \hat{h}_{i_k}(2^k \nu) \hat{h}_{j_k} \left(2^k (\omega - \nu) \right) \right]$$

$$\cdot \left[\hat{h}_{i_0+j_0}(\omega) + (-1)^{i_0} e^{-j\nu} \hat{h}_{i_0+j_0}(\omega - 2\nu) \right] d\nu$$

$$= \frac{1}{2} \sum_{\boldsymbol{i}} \sum_{\boldsymbol{j}} \hat{h}_{i_0+j_0}(\omega) \int_{-\pi}^{\pi} \hat{v}_{\boldsymbol{i}}^x(2^I \nu) \hat{v}_{\boldsymbol{j}}^x \left(2^I (\omega - \nu) \right)$$

$$\cdot \left[\prod_{k=1}^{I-1} \hat{h}_{i_k}(2^k \nu) \hat{h}_{j_k} \left(2^k (\omega - \nu) \right) \right] d\nu,$$

where we have used the fact that $\int_{-\pi}^{\pi} e^{-j2^k \nu} \hat{f}(\nu) d\nu = 0$ for all $\hat{f}(\nu) \in L(\mathbb{R}/2^{-k}\pi)$ whenever $k \geq 0$, as $e^{-j(2^k \nu - \pi)} \hat{f}(\nu - 2^{-k}\pi) = -e^{-j2^k \nu} \hat{f}(\nu)$. By recursion over k, the above reduces to

$$\widehat{(x \cdot y)}(\omega) = \frac{1}{2^K} \sum_{\boldsymbol{i}} \sum_{\boldsymbol{j}} \left[\prod_{k=0}^{K-1} \hat{h}_{i_k+j_k}(2^k \omega) \right]$$

$$\cdot \int_{-\pi}^{\pi} \hat{v}_{\boldsymbol{i}}^x(2^I \nu) \hat{v}_{\boldsymbol{j}}^x \left(2^I (\omega - \nu) \right)$$

$$\cdot \left[\prod_{k=K}^{I-1} \hat{h}_{i_k}(2^k \nu) \hat{h}_{j_k} \left(2^k (\omega - \nu) \right) \right] d\nu$$

$$= \frac{1}{2^{K+1}} \sum_{\boldsymbol{i}} \sum_{\boldsymbol{j}} \left[\prod_{k=0}^{K} \hat{h}_{i_k+j_k}(2^k \omega) \right]$$

$$\cdot \int_{-\pi}^{\pi} \hat{v}_{\boldsymbol{i}}^x(2^I \nu) \hat{v}_{\boldsymbol{j}}^x \left(2^I (\omega - \nu) \right)$$

$$\cdot \left[\prod_{k=K+1}^{I-1} \hat{h}_{i_k}(2^k \nu) \hat{h}_{j_k} \left(2^k (\omega - \nu) \right) \right] d\nu \tag{17}$$

$$= \cdots = \frac{1}{2^I} \sum_{\boldsymbol{i}} \sum_{\boldsymbol{j}} \left[\prod_{k=0}^{I-1} \hat{h}_{i_k+j_k}(2^k \omega) \right]$$

$$\cdot \left[\hat{v}_{\boldsymbol{i}}^x(2^I \omega) \star_\omega \hat{v}_{\boldsymbol{j}}^y(2^I \omega) \right].$$

Note that (17) takes the form of a multi-level inverse filterbank transform, as per (15). As the Haar filterbank transform is one-to-one and onto, $v_{\boldsymbol{i}}^{xy}$ is thus uniquely defined by

$$\hat{v}_{\boldsymbol{i}}^{xy}(\omega) = \frac{1}{2^I} \sum_{\boldsymbol{j}} \left[\hat{v}_{\boldsymbol{i}+\boldsymbol{j}}^x(\omega) \star_\omega \hat{v}_{\boldsymbol{j}}^y(\omega) \right],$$

which agrees with the claim of the theorem. ∎

Figure 9 illustrates the corresponding "rewiring" of filterbank subbands, in which $v_{\boldsymbol{i}}^x[n]$ and $v_{\boldsymbol{i}}^y[n]$ are coupled together to yield $v_0^{xy}[n]$, and $v_{\boldsymbol{i}'}^x[n]$ and $v_{\boldsymbol{i}}^y[n]$ are combined to produce
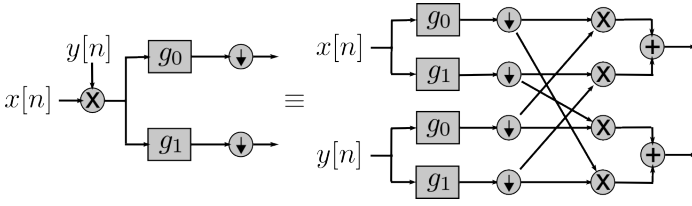
Fig. 9. Illustration of Theorem 3, showing the correspondence between time-domain multiplication and "logical convolution" of filterbank subbands.

v_1^{xy}.

Remark 3.1 (Logical Convolution): By restricting x and y be finite-dimensional, we recover the so-called logical convolution theorem [14] as a special case of Theorem 3. This is easily seen by considering an order-2^I Walsh sequence $\vec{\phi}_{\boldsymbol{i}} \in \mathbb{R}^{2^I}$ and its Abelian structure:

$$\mathrm{diag}(\vec{\phi}_{\boldsymbol{i}})\vec{\phi}_{\boldsymbol{j}} = \vec{\phi}_{\boldsymbol{i}+\boldsymbol{j}}, \quad \boldsymbol{i}, \boldsymbol{j} \in \{\mathbb{Z}_2\}^I. \tag{18}$$

Orthogonality of the Walsh basis sets implies that any $\vec{x} \in \mathbb{R}^{2^I}$ can be expanded in terms of its Walsh-Hadamard coefficients $\left\langle \vec{\phi}_{\boldsymbol{i}}, \vec{x} \right\rangle = \vec{\phi}_{\boldsymbol{i}}^T \vec{x}$ as $\vec{x} = 2^{-I} \sum_{\boldsymbol{j}} \left\langle \vec{\phi}_{\boldsymbol{j}}, \vec{x} \right\rangle \vec{\phi}_{\boldsymbol{j}}$, and hence the group homomorphism of (18) yields the desired relation for all $\vec{x}, \vec{y} \in \mathbb{R}^{2^I}$:

$$\left\langle \vec{\phi}_{\boldsymbol{i}}, \mathrm{diag}(\vec{x})\vec{y} \right\rangle = \frac{1}{2^{2I}} \sum_{\boldsymbol{j},\boldsymbol{j}'} \left\langle \vec{\phi}_{\boldsymbol{j}}, \vec{x} \right\rangle \left\langle \vec{\phi}_{\boldsymbol{j}'}, \vec{y} \right\rangle \left\langle \vec{\phi}_{\boldsymbol{i}}, \mathrm{diag}(\vec{\phi}_{\boldsymbol{j}})\vec{\phi}_{\boldsymbol{j}'} \right\rangle$$
$$= \frac{1}{2^I} \sum_{\boldsymbol{j}} \left\langle \vec{\phi}_{\boldsymbol{j}}, \vec{x} \right\rangle \left\langle \vec{\phi}_{\boldsymbol{i}+\boldsymbol{j}}, \vec{y} \right\rangle.$$

B. Localized Modulation and Connection to Reverse-Ordered Subband Structure

We conclude this section by interpreting the result of Theorem 3 in terms of amplitude modulation and sampling.

Remark 3.2 (Multi-Level ROSS for Haar Filterbank Transform): Suppose that we set $v_{(0,\ldots,0,0)}^y[n] = v_{(0,\ldots,0,1)}^y[n] = 2^{I-1}$ for all n, and $v_{\boldsymbol{i}}^y[n] = 0$ otherwise, thus yielding a Dirac comb. Then Theorem 3 agrees precisely with Corollary 2.3:

$$\left(v_{\boldsymbol{j}}^x \circledast_{\boldsymbol{j}} v_{\boldsymbol{j}}^y\right)_{\boldsymbol{i}}[n] = \frac{1}{2}\left(v_{\boldsymbol{i}}^x[n] + v_{\boldsymbol{i}'}^x[n]\right).$$

Remark 3.3 (Generalized Subsampling): More generally, suppose $y[n] \in \{0,1\}$ is a sampling mask of any kind. Then it may be seen from Figure 9 that the subsampled signal $x[n]y[n]$ is aliased if $v_0^x[n]v_0^y[n]$ and $v_1^x[n]v_1^y[n]$ (or, $v_0^x[n]v_1^y[n]$ and $v_0^x[n]v_1^x[n]$) are simultaneously supported.

Remark 3.4 (Localized Modulation): Consider Figure 9 again and suppose at time $n = 0$, we have that $v_0^y[n] = 0$ and $v_1^y[n] = 1$. Then $v_0^x[n]$ is "modulated" to $v_1^{xy}[n]$. This is similar to Fourier amplitude modulation, in which case the energy of the modulated signal is concentrated around a chosen carrier frequency; however, a representation based on Theorem 3 is amenable to temporally local processing. For example, suppose at time $n = 1$, we take $v_0^y[n] = 1$ and $v_1^y[n] = 0$; then $v_0^x[n]$ is mapped to $v_0^{xy}[n]$ instead of $v_1^{xy}[n]$. In other words, this filterbank interpretation of *localized modulation*—illustrated in Figure 10—is ideal for tracking modulation when the "carrier" $y[n]$ is allowed to change over time.
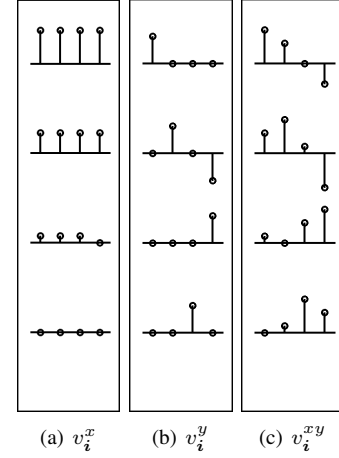

(a) $v_{\boldsymbol{i}}^x$ (b) $v_{\boldsymbol{i}}^y$ (c) $v_{\boldsymbol{i}}^{xy}$

Fig. 10. Pictorial illustration of *localized modulation* in 2-level filterbank domain. Time-domain multiplication of x and y, represented by their filterbank coefficients in (a) and (b), results in subband convolution, shown in (c); "rewiring" is evident in comparing (a) and (c). Exact recovery of $v_{\boldsymbol{i}}^x[n]$ from $v_{\boldsymbol{i}}^{xy}[n]$ is possible when the supports of $v_{\boldsymbol{i}+\boldsymbol{j}}^x[n]$ are mutually exclusive for all $\boldsymbol{i}$ and $\boldsymbol{j}$ corresponding to nonzero $v_{\boldsymbol{i}}^x[n]$ and $v_{\boldsymbol{j}}^y[n]$.

Formally, we are concerned with characterizing a sum $z[n] = \sum_k x_k[n]y_k[n]$ of modulated sequences x_k. When the "envelope function" $y_k[n]$ is chosen carefully, then it follows from Theorem 3 that these signals are recoverable.

Proposition 3.1 (Localized Amplitude Modulation): Suppose $y_k[n]$ is defined by a sequence of index values $\boldsymbol{j}_k \in \{\mathbb{Z}_2\}^I$ and Haar filterbank coefficients: $v_{\boldsymbol{i}}^{y_k}[n] = \delta(\boldsymbol{i}, \boldsymbol{j}_k[n])$. Then $x_k[n]$ is recoverable from $z[n] = \sum_k x_k[n]y_k[n]$ when the supports of $v_{\boldsymbol{i}+\boldsymbol{j}_k[n]}^{x_k}[n]$ are mutually exclusive for all $\boldsymbol{i}$ and k.

Proof: By the subband convolution result of Theorem 3,

$$v_{\boldsymbol{i}}^z[n] = \sum_k v_{\boldsymbol{i}}^{x_k y_k}[n] = \sum_k \left(v_{\boldsymbol{j}}^{x_k} \circledast_{\boldsymbol{j}} v_{\boldsymbol{j}}^{y_k}\right)_{\boldsymbol{i}}[n] = \sum_k v_{\boldsymbol{i}+\boldsymbol{j}_k[n]}^{x_k}[n]$$

However, by the assumed mutual exclusivity of the supports of $v_{\boldsymbol{i}+\boldsymbol{j}_k[n]}^{x_k}[n]$, it follows that

$$v_{\boldsymbol{i}}^z[n] = \begin{cases} v_{\boldsymbol{i}+\boldsymbol{j}_k[n]}^{x_k}[n] & \text{if there exists } k \text{ with nonzero } v_{\boldsymbol{i}+\boldsymbol{j}_k[n]}^{x_k} \\ 0 & \text{otherwise,} \end{cases}$$

and thus we conclude that $v_{\boldsymbol{i}}^{x_k}[n] = v_{\boldsymbol{i}+\boldsymbol{j}_k[n]}^z[n]$ whenever $v_{\boldsymbol{i}}^{v_k}[n]$ is nonzero. ∎

IV. DISCUSSION: IMPLICATIONS FOR SIGNAL ANALYSIS

The preceding two sections have explored properties of reverse-order and convolution subband structure (ROSS and SCS) in filterbanks, and shown their relation to the concepts of localized aliasing and modulation. We now discuss the practical implications of these results for signal analysis, and provide two brief demonstrations that "rewiring" filterbank diagrams in the manner of ROSS and SCS can enable new solutions to problems involving subsampled data corrupted by additive or multiplicative noise. As many scientific and engineering applications give rise to inverse problems involving subsampled and/or noisy data, and since filterbanks are the tool of choice for many signal and image processing tasks, it

is natural to analyze the data likelihoods resulting from these problems directly in the filterbank coefficient domain.

A. Filterbank-Domain Likelihoods via ROSS and SCS

While data likelihoods often do not admit straightforward closed-form expressions through traditional filterbank analysis, the ROSS and SCS concepts provide a new way to characterize signals subject to aliasing or signal-dependent noise effects directly in the filterbank coefficient domain, by virtue of the associated filterbank rewiring techniques. The expression of filterbank data likelihoods is key to solving signal reconstruction and enhancement problems in this context; as signal acquisition models, these likelihoods may be coupled with regularization terms that encourages parsimony as a means of signal modeling, reflected through prior probability densities on filterbank coefficients, or equivalently through terms that explicitly penalize complexity. To this end, the following two corollaries show how explicit likelihood formulations follow directly from application of the ROSS and SCS concepts introduced earlier.

Corollary 4.1 (Noisy, Subsampled Data Likelihood): Fix $x \in \ell^2(\mathbb{Z})$ as the signal of interest, and let ξ comprise samples of white Gaussian noise of variance σ^2. Suppose then that we observe *subsampled, noisy* data $y = x_s + \xi_s$ and subsequently apply a *unitary* filterbank transform; then it follows from the localized aliasing relation of Theorem 2 that the analysis filterbank coefficients of y satisfy

$$v_i^y[n] = \frac{v_i^x[n] + (-1)^{i_0} w_{i'}^x[n]}{2} + \frac{v_i^\xi[n] + (-1)^{i_0} w_{i'}^\xi[n]}{2},$$

and hence each admits a Normal likelihood with mean $\left(v_i^x[n] + (-1)^{i_0} w_{i'}^x[n]\right)/2$ and variance $\sigma^2/2$.

Corollary 4.2 (Multiplicative Noise Data Likelihood): Suppose instead that the observation model $y[n] = x[n] + x[n]\xi[n]$ is in force. Then the subband convolution structure of Theorem 3 implies the filterbank coefficient relation

$$v_i^y[n] = v_i^x[n] + \left(v_j^x[n] \circledast_j v_j^\xi[n]\right)_i,$$

and hence the likelihood form of $v_i^y[n]$ is multivariate Normal with mean $v_i^x[n]$, where the covariance of $v_i^y[n]$ and $v_j^y[n]$ is given by $\sigma^2(v_k^x \circledast_k v_k^x)_{i+j}$.

B. Proof of Concept: Application to Image Interpolation and Denoising

The likelihood expressions of Corollaries 4.1 and 4.2 above extend straightforwardly to the case of separable two-dimensional filterbank transforms, which in turn are typically employed in imaging applications. Thus, to illustrate the practical applicability of these results, we now undertake two proof-of-concept experiments that are representative of problems frequently encountered in digital imaging, and for which our ROSS and SCS characterizations—in contrast to standard approaches—yield closed-form likelihood expressions for the corresponding filterbank coefficients.

The first of these—image interpolation in the presence of noise—is made difficult by the fact that low- and high-frequency filterbank subbands interact with one another as well as with the noise itself; the "rewiring" expression of Corollary 4.1 in turn provides a closed-form likelihood expression for the filterbank coefficients. In the second experiment, we consider the similarly difficult problem of mitigating *multiplicative* noise; in this case, Corollary 4.2 yields the corresponding likelihood.

As filterbank coefficients of images typically exhibit sparsity [15], one natural approach to utilize these likelihoods through a Bayesian framework, in which transform coefficients of the underlying image x are modeled as random variables $v_i^X[n]$ taking zero-mean, symmetric, and unimodal "heavy-tailed" distributions that exhibit super-Gaussian tail behavior [16], [17]. We assume such a prior distribution here, and evaluate posterior means numerically via Monte Carlo averages.

We follow typical practice in approximating the overall joint posterior distribution of all filterbank coefficients by a product of marginal distributions, where each marginal posterior is associated with a particular subband. In turn, the ℓ^2-optimal estimator of filterbank coefficients $v_i^X[n]$ corresponding to the ith subband given the corresponding data coefficients $v_i^y[n]$ is given by

$$\mathbb{E}[v_i^X | v_i^y] = \frac{\int v_i^x p(v_i^y | v_i^x) p(v_i^x) dv_i^x}{p(v_i^y)}; \tag{19}$$

the corresponding synthesis filterbank in turn allows reconstruction of the estimated image.

We first consider a well-known 8-bit test image that has been artificially downsampled and degraded with additive white Gaussian noise of variance 400 to yield a signal-to-noise ratio (SNR) of 16.77 dB relative to x_s (or 1.22 dB relative to x), as shown in Figures 11(a) and 11(b). Figure 11(c) shows the corresponding image reconstruction, which retains much of sharpness of the image edges and textures while suppressing noise, resulting in an SNR gain of 3.81 dB. For purposes of comparison, Figure 11(d) shows the result of the recently proposed simultaneous interpolation and denoising method of [18], which yields an SNR gain of 3.55 dB; this reconstruction exhibits edges that are more strongly preserved, but at the expense of greater smoothing of image textures.

In our second experiment, we consider a synthetic aperture radar (SAR) image, available at www.sandia.gov/radar; as may be seen from Figure 12(a), such images suffer from the effects of multiplicative noise [19]. Figure 12(b) shows the enhanced image resulting from a "rewiring" approach, which exhibits reduced noise in smooth and textured regions, and avoids the introduction of artifacts. In contrast, Figure 12(c) illustrates the standard approach: application of a logarithmic transformation to the data, followed by an additive denoising technique (here the well-known method of [16]) and subsequent exponentiation of the result. Not only are Bayes optimality properties of [16] lost in the exponentiation transformation back to the pixel domain, but also substantial artifacts are seen to result from this standard approach.

(a) Original test image

(b) Subsampled, noisy test image

(c) "Rewiring" reconstruction

(d) Reconstruction via the method of [18]

Fig. 11.   Example of noisy image interpolation via the ROSS technique of Section II: The first row shows a full-resolution 8-bit test image (a), along with a subsampled version that has been degraded with additive white Gaussian noise of variance 400 (b). The bottom row shows a posterior mean reconstruction based on the filterbank-domain likelihood of Corollary 4.1 and a heavy-tailed prior distribution on filterbank coefficients (c), along with a reconstruction according to the recently proposed method of [18], shown for comparison (d).

C. Concluding Remarks

In conclusion, we have shown in this article how filterbank "rewirings," corresponding to compositions of convolution, modulation, and downsampling operators, admit expressions of *localized* aliasing and modulation, in directly analogy to the global setting of Fourier analysis. In addition to establishing a number of results that formalize reverse-order and convolution subband structures in filterbank transforms in Sections II and III, respectively, we have demonstrated in this section how these concepts in turn enable the establishment of closed-form likelihood functions for the direct filterbank analysis of signals subject to degradations such as missing data, spatially or temporally multiplexed data acquisition, or signal-dependent noise, such as are often encountered in practical signal processing applications.

(a) SAR image showing "speckled noise" (b) "Rewiring" enhancement (c) Enhancement via the method of [16], applied after logarithmic transformation
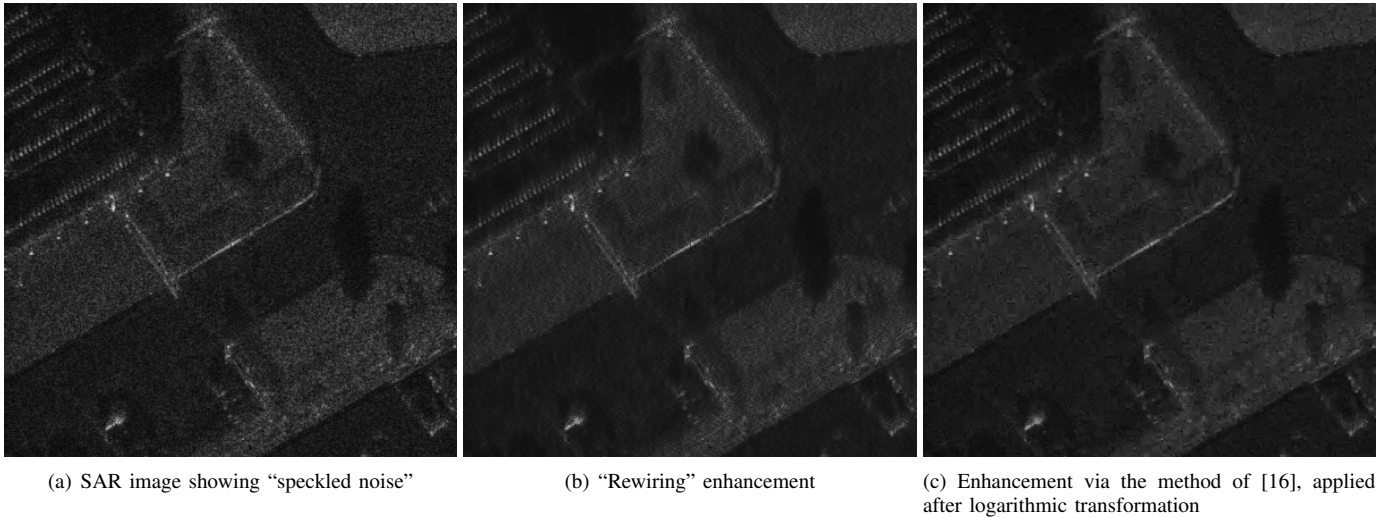
Fig. 12. Example of multiplicative noise mitigation via the SCS technique of Section III: Panel (a) shows a portion of SAR imagery data in which noise is visibly present. Panel (b) shows an enhancement based on the filterbank-domain likelihood of Corollary 4.2 and a heavy-tailed prior distribution on filterbank coefficients, with panel (c) showing for comparison an enhancement according to the method of [16], designed for additive noise and applied after a variance-stabilizing logarithmic transformation.

kindly providing their code for the purpose of comparative evaluation.

REFERENCES

[1] S. Mallat, *A Wavelet Tour of Signal Processing*, Academic Press, Burlington, MA, third edition, 2009.

[2] G. Strang and T. Nguyen, *Wavelets and Filter Banks*, Wellesley-Cambridge Press, Wellesley, MA, 1996.

[3] D.L. Donoho, "Compressed sensing," *IEEE Trans. Info. Theory*, vol. 52, pp. 1289–1306, 2006.

[4] E.J. Candés, "Compressive sampling," in *Proc. Intl. Congr. Mathem.*, 2006, vol. 3, pp. 1433–1452.

[5] E.J. Candés and T. Tao, "Near-optimal signal recovery from random projections: Universal encoding strategies?," *IEEE Trans. Info. Theory*, vol. 52, pp. 5406–5425, 2006.

[6] E.J. Candés, J. Romberg, and T. Tao, "Robust uncertainty principles: Exact signal reconstruction from highly incomplete frequency information," *IEEE Trans. Info. Theory*, vol. 52, pp. 489–509, 2006.

[7] J. Haupt and R. Nowak, "Signal reconstruction from noisy random projections," *IEEE Trans. Info. Theory*, vol. 52, pp. 4036–4048, 2006.

[8] Y. Eldar and T. Michaeli, "Beyond bandlimited sampling," *IEEE Signal Process. Mag.*, vol. 26, pp. 48–68, 2009.

[9] G. G. Walter, "A sampling theorem for wavelet subspaces," *IEEE Trans. Info. Theory*, vol. 38, pp. 881–884, 1992.

[10] X.-G. Xia and Z. Zhang, "On sampling theorem, wavelets, and wavelet transforms," *IEEE Trans. Signal Process.*, vol. 41, pp. 3524–3535, 1993.

[11] P.P. Vaidyanathan, "Generalizations of the sampling theorem: Seven decades after Nyquist," *IEEE Trans. Circuits Syst. I*, vol. 48, pp. 1094–1109, 2001.

[12] P.P. Vaidyanathan and V.C. Liu, "Classical sampling theorems in the context of multirate and polyphase digital filter bank structures," *IEEE Trans. Acoust. Speech Signal Process.*, vol. 36, pp. 1480–1495, 1988.

[13] M. Smith and T. Barnwell, "A procedure for designing exact reconstruction filter banks for tree-structured subband coders," in *Proc. IEEE Intl. Conf. Acoust. Speech Signal Process.*, 1984, vol. 9, pp. 421–424.

[14] B. Kennett, "A note on the finite Walsh transform," *IEEE Trans. Info. Theory*, vol. 16, pp. 489–491, 1970.

[15] M. S. Crouse, R. D. Nowak, and R. G. Baraniuk, "Wavelet-based statistical signal processing using hidden Markov models," *IEEE Trans. Signal Process.*, vol. 46, pp. 886–902, 1998.

[16] J. Portilla, V. Strela, M.J. Wainwright, and E.P. Simoncelli, "Image denoising using scale mixtures of Gaussians in the wavelet domain," in *Proc. IEEE Intl. Conf. Image Process.*, 2003, vol. 12, pp. 1338–1351.

[17] I. W. Selesnick, "Laplace random vectors, Gaussian noise, and the generalized incomplete Gamma function," in *Proc. IEEE Intl. Conf. Image Process.*, 2006, pp. 2097–2100.

[18] L. Zhang and X. Li, "Directional interpolation of noisy images," in *Proc. IEEE Intl. Conf. Image Process.*, 2008, pp. 633–636.

[19] A. Achim, P. Tsakalides, and A. Bezerianos, "SAR image denoising via Bayesian wavelet shrinkage based on heavy-tailed modeling," *IEEE Trans. Geosci. Remote Sens.*, vol. 41, pp. 1773–1784, 2003.